Electronic Supplementary Material (ESI) for RSC Advances.

SUPPLEMENTARY MATERIAL

A new approach to study semi-coordination using two 2–methyl–5–nitroimidazole copper(II) complexes of biological interest as a model system

*Lucas G. Fachini[a], Gabriel B. Baptistella[a], Kahoana Postal[a], Francielli S. Santana[a], Emanuel M. de Souza[b], Eduardo L. Sá[a], Ronny R. Ribeiro[a], Giovana G. Nunes[a]**

[a]*Departamento de Química, UFPR, Curitiba-PR, Brasil.*

[b]*Departamento de Bioquímica e Biologia Molecular, UFPR, Curitiba-PR, Brasil*

Table S1. Comparison between bond lengths (Å) and angles (°) obtained through DRX-single crystal and DFT calculations for product **1** B3LYP/LANL2DZ

	DRX	DFT
	Bond lengths / Å	
Cu–O(1w)	1.94988	1.94988
Cu–O(1)	2.60642	2.60642
Cu–N(2)	1.99355	2.02068
O(1)–N(1)	1.23795	1.30158
O(2)–N(1)	1.21906	1.26275
C(3)–N(1)	1.42402	1.43568
C(3)–C(4)	1.35937	1.38636
C(4)–N(3)	1.35545	1.38146
C(2)–N(3)	1.35483	1.38614
C(2)–N(2)	1.32490	1.35239
C(1)–C(2)	1.48010	1.49540
	Angles / º	
O(1w)–Cu–O(1w)^{i}	180.0	179.685
N(2)–Cu–N(2)^{i}	180.0	177.799
O(1)–Cu-O(1)^{i}	180.0	163.308
O(1)–Cu–O(1w)	88.150	98.947
N(2)–Cu–O(1w)	90.180	88.943
O(1)–Cu–N(2)	69.917	72.046
O(1)–Cu–N(2)^{i}	110.083	108.172
Cu–O(1)–N(1)	108.579	107.862
O(1)–N(1)–O(2)	124.228	124.299
O(2)–N(1)–C(3)	118.368	118.901
N(2)–C(3)–N(1)	120.085	121.852
N(1)–C(3)–C(4)	128.566	127.863
C(3)–C(4)–N(3)	104.140	104.449
C(2)–N(3)–C(4)	109.614	110.388
N(2)–C(2)–N(3)	109.589	108.058
N(3)–C(2)–C(1)	124.578	124.175
C(2)–N(2)–C(3)	105.306	106.833
N(2)–C(2)–C(1)	125.822	127.767
Cu–N(2)–C(2)	130.584	131.608
Cu–N(2)–C(3)	123.598	121.396

Table S2. Comparison between bond lengths (Å) and angles (°) obtained through DRX-single crystal and DFT calculations for product **2** B3LYP/LANL2DZ

	DRX		DFT
		Bond lengths / Å	
Cu–O(1N4)	1.99492		1.99491
Cu–O(1)	2.59367		2.59367
Cu–N(2)	1.97291		1.99290
N(1)–O(1)	1.23134		1.28390
N(1)–O(2)	1.22734		1.27715
N(1)–C(3)	1.41980		1.43409
C(3)–C(4)	1.35367		1.35593
C(2)–N(3)	1.35225		1.38936
C(2)–N(2)	1.32724		1.33909
C(1)–C(2)	1.47443		1.49083
N(4)–O(1N4)	1.28877		1.36599
N(4)–O(2N4)	1.22059		1.29077
N(4)–O(3N4)	1.23688		1.27127
		Angles / º	
O(1N4)–Cu–O(1N4)^{I}	180.0		179.677
O(1)–Cu–O(1)^{i}	180.0		179.685
N(2)–Cu–N(2)^{i}	180.0		179.859
O(1N4)–Cu–O(1)	99.492		102.062
O(1N4)–Cu–N(2)	86.483		87.640
O(1)–Cu–N(2)	70.911		71.686
N(2)–Cu–O(1)^{i}	109.089		108.432
Cu–O(1N4)–N(4)	121.150		121.219
O(1N4)–N(8)–O(2N4)	120.487		118.200
O(1N4)–N(4)–O(3N4)	117.018		117.327
O(2N4)–N(4)–O(3N4)	122.495		124.474
Cu–O(1)–N(1)	107.401		107.173
O(1)–N(1)–O(2)	124.115		124.837
O(1)–N(1)–C(3)	118.081		117.111
N(1)–C(3)–N(2)	120.650		120.792
N(1)–C(3)–C(4)	128.354		128.587
C(3)–C(4)–N(3)	104.750		104.020
C(4)–N(3)–C(2)	109.450		109.888
N(2)–C(2)–N(3)	109.295		108.115
C(3)–N(2)–C(2)	105.544		107.386
N(3)–C(2)–C(1)	124.415		125.377
N(2)–C(2)–C(1)	126.290		126.506
Cu–N(2)–C(2)	131.698		130.308
Cu–N(2)–C(3)	122.621		122.182

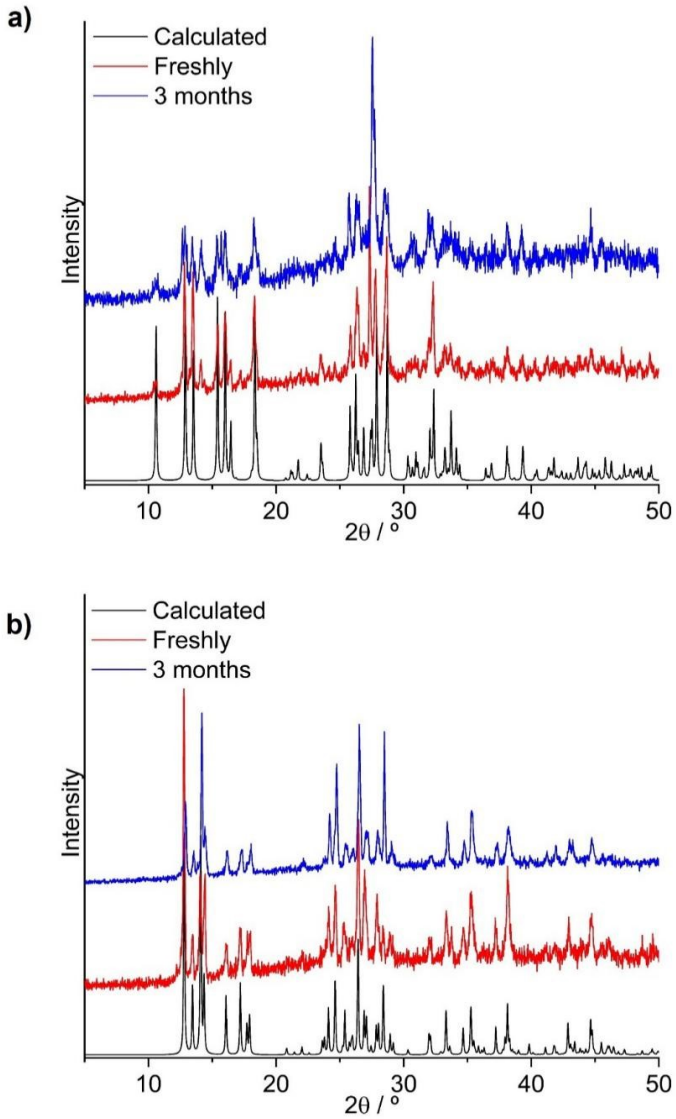

Figure S1. Powder X-ray diffraction patterns recorded (black line) and calculated (red line) for **(a)** $[Cu(2mni)_2(H_2O)_2](NO_3)_2{\cdot}2H_2O$ (**1**) and **(b)** $[Cu(2mni)_2(NO_3)_2]$ (**2**).

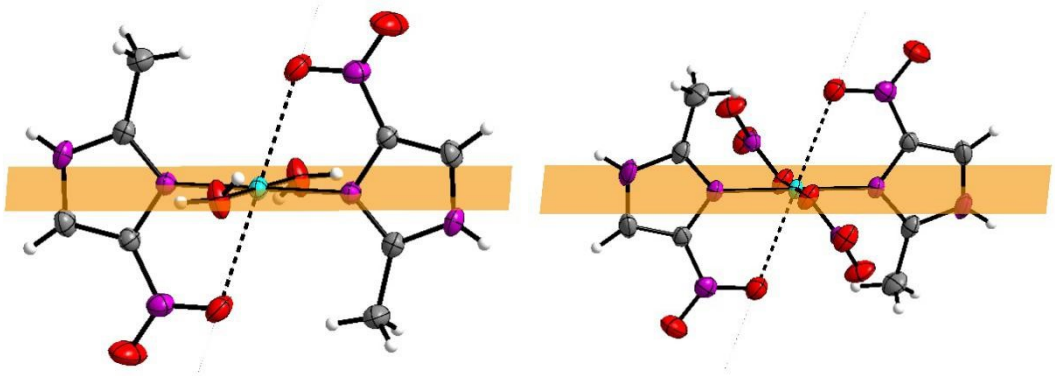

Figure S2. Plans obtained for **(a)** $[Cu(2mni)_2(H_2O)_2](NO_3)_2(H_2O)_2$ (**1**) and **(b)** $[Cu(2mni)_2(NO_3)_2]$ (**2**).

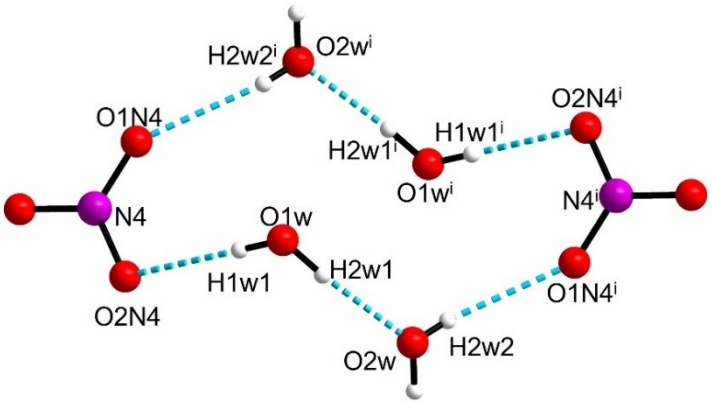

Figure S3. Ring forming by the hydrogens bond in **1**.

Table S3. Selected structural parameter for compounds analogous to **1** and **2**

	Compound	Cu–O_{axial} / Å	Ring members	Tetragonality parameter (τ)	Ref.
	1	2.606(14)	5	0.756	#
	2	2.594(15)	5	0.764	#
A	$[Cu(emizco)_2(H_2O)_2](NO_3)_2$	2.519(15)	5	0.789	1
B	$[Cu(tdaH_2)_2(H_2O)_2]\cdot 2H_2O$	2.490(2)	5	0.792	2
C	$[Cu(cpt)_2(H_2O)_2](MeOH)_2$	2.463(2)	5	0.804	3
D	$[Cu(atNO_2EtOH)_2(H_2O)_2]$	2.405(2)	6	0.823	4
E	$[Cu(C_2H_3N_6O_2)_2(H_2O)_2]\cdot 2H_2O$	2.393(1)	6	0.829	5
F	$[Cu(atNO_2EtCl)_2(H_2O)_2]\cdot 2H_2O$	2.367(1)	6	0.838	4
G	$[Cu(ron)_2(H_2O)_2](NO_3)_2$	2.336(3)	7	0.849	6
H	$[Cu(C_2H_3N_6O_2)_2(H_2O)_2](MeOH)_2$	2.326(2)	6	0.851	5

Where: TDAH2 = 1,2,3-triazole4,5dicarboxylic acid; CPT = 1-(3,5-dinitro1H-pyrazol-4-yl)-3-nitro-1H-1,2,4-triazol-5-amine; C2H3N6O2 = 1-methyl-5-nitriminotetrazole; emizco = ethyl 5-methyl-4-imidazolecarboxylate; AtNO2EtOH = 1-(2-Hydroxyethyl)-5-nitriminotetrazole and AtNO2EtOH = 1-(2-Chloroethyl)-itriminotetrazole; ron = (1-methyl-5-nitro-1H-imidazol-2-yl)methylcarbamate. #This work.

Table S4. Product **1** hydrogen bonds list, in Ångstroms (Å) and angles in degrees (°)

D–H...A	d(D–H)	d(H...A)	d(D...A)	<(DHA)
O(1W)–H(1W1)...O(2N4)	0.76(3)	2.02(3)	2.778(2)	179(3)
O(1W)–H(2W1)...O(2W)	0.84(2)	1.80(3)	2.6409(19)	175(2)
C(1)–H(1B)...O(1)^{i}	0.90(3)	2.61(3)	3.417(2)	151(2)
C(1)–H(1C)...O(2)^{ii}	0.90(3)	2.64(3)	3.410(3)	144(2)
N(3)–H(1N3)...O(3N4)^{iii}	0.75(2)	2.29(2)	2.924(2)	143(2)
C(4)–H(4)...O(1)^{iv}	0.91(2)	2.52(2)	3.416(2)	166.2(16)
O(2W)–H(1W2)...O(3N4)^{ii}	0.82(3)	2.09(3)	2.866(2)	159(3)
O(2W)–H(2W2)...O(1N4)^{v}	0.71(3)	2.19(3)	2.872(2)	161(3)

Symmetry transformations used to generate equivalent atoms:
(i) –x+1,–y+1,–z+1 (ii) x,–y+3/2,z–1/2 (iii) –x+1,–y+2,–z+1
(iv) –x+1,y+1/2,–z+3/2 (v) –x+2,–y+1,–z+1

Table S5. Product **2** hydrogen bonds list, in Ångstroms (Å) and degrees (°)

D–H...A	d(D–H)	d(H...A)	d(D...A)	<(DHA)
N(3)–H(3N3)...O(3N4)^{ii}	0.84(3)	2.00(3)	2.837(2)	173(3)

Symmetry transformations used to generate equivalent atoms:
(ii) –x+1/2,y–1/2,–z+1/

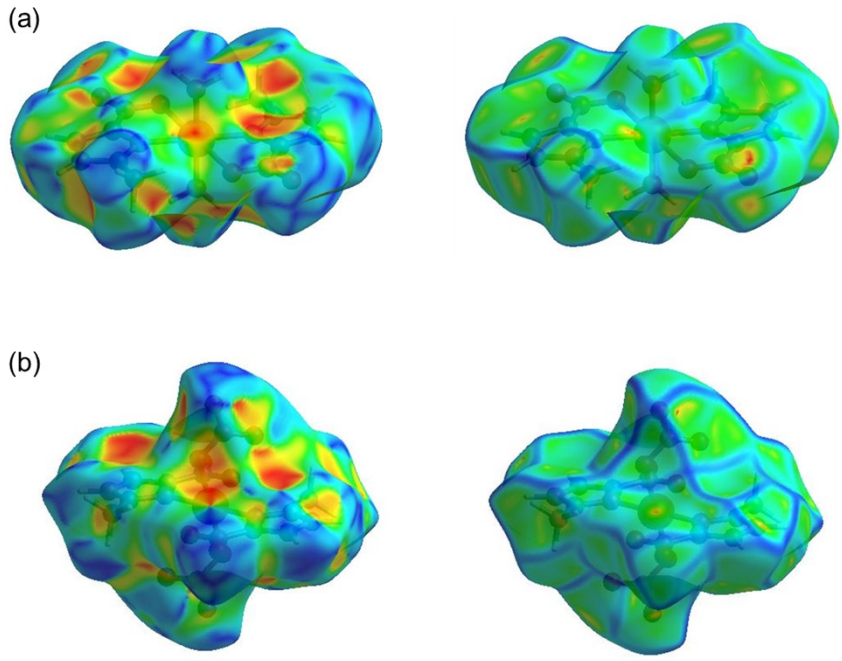

Figure S4. Hirshfeld surfaces mapped for shape index and curvedness, respectively, for (a) **1** and (b) **2**. This method also allows us to calculate unique shape properties for the molecules, as shape index and curvedness. The shape index can show subtle changes in the molecule surface shape, where the blue parts suggest convex regions and the red, the concave regions and are present in both **1** and **2** surface, being more evident at product **2**. A slight difference is also observed in the curvedness surface of the products, with the predominance of green areas of low values of curvedness in **1** when compared to **2**. Whereas sharp curvature areas assigned by the blue color are more defined in **2**. These structural and conformational differences can be mainly attributed to the shape and size of the ligands, once the water molecules at **1** are smaller than the nitrate group of product **2** leading to a less bulky structure.

Table S6. Percentage contributions from the other different interatomic contacts to the Hirshfeld surface of **1** and **2**

	Product **1**	Product **2**
Contact	**Contribution / %**	**Contribution / %**
H···O/O···H	60.8	51.4
N···H/H···N	2.0	6.4
C···H/H···C	2.3	9.8
C···N/N···C	1.4	0.0
N···O/O···N	3.6	8.0
C···O/O···C	3.7	2.2
H···H	22.0	9.5

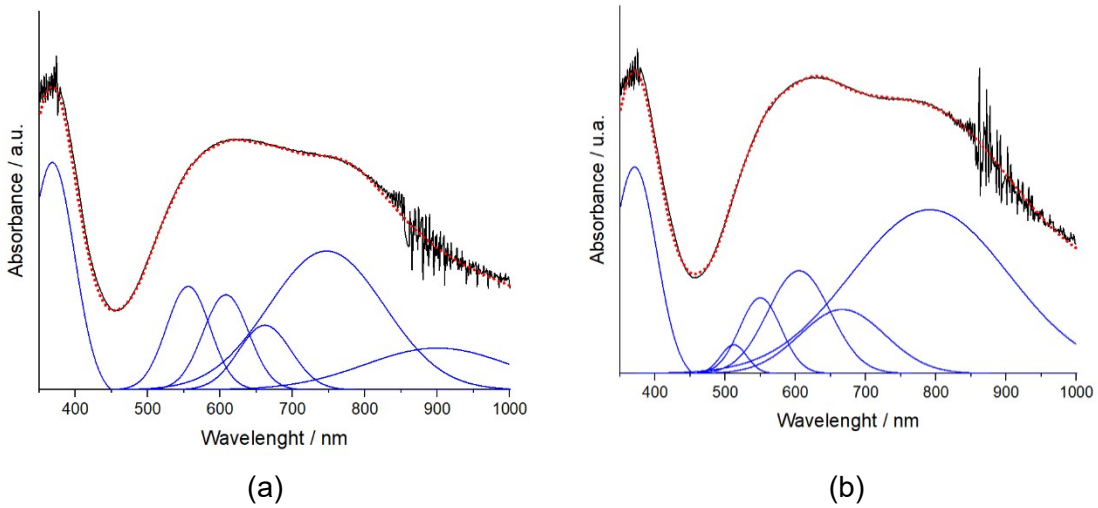

Figure S5. Solid-state UV-Vis spectrum for compounds **1** (a) and **2** (b).

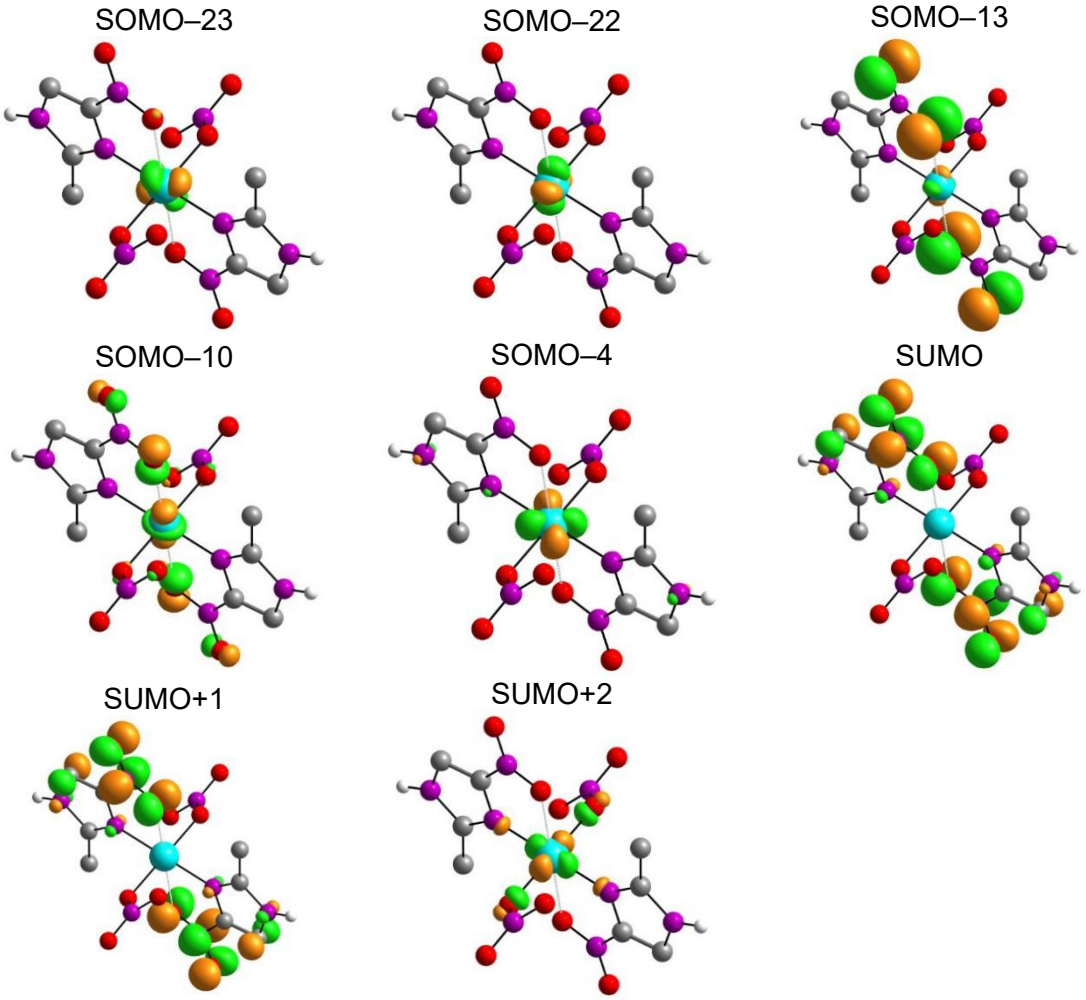

Figure S6. Representation of selected frontier molecular orbitals involved in the UV-vis absorptions calculated for **2**. SUMO and SOMO denotes the single unoccupied molecular orbital and the single occupied molecular orbital, respectively.

Table S7. Tentative assignments for the FTIR (cm^{-1}) spectra registered and calculated for product **1** and **2**

Tentative assignments	**1** Experimental	**1** Calculated	**2** Experimental	**2** Calculated
ν(O–H)	3180	3320	–	–
ν(N–H)	3180	3320	3560	3669
ν_s(C–H)	3084	3058	3117	3157
ν_{as}(N–O)	1587	1602	1595	1609
$\nu_s(C{=}N)_{ring}$	1543 and 1477	1566 and 1509	1541 and 1518	1577 and 1529
$\nu_{as}(NO_3)_{nitrate}$	1383	1379	–	–
$\nu_s(NO_2)_{nitrate}$	–	–	1246	1222
ν_s(N–O)	1383	1379	1385	1409
$\nu_s(NO_3)_{nitrate}$	1034	1067	–	–
$\nu_s(C{=}N)_{ring}$	1300 and 1240	1306 and 1202	1246	1222
δ(C–N–C)	1115	1148	1115	1137
$\delta(NO_3)$	748	732	–	–
$\delta(NO_2)$	–	–	748	741
δ(C–H)	675	645	675	686

ν = stretching, ν_{as} = asymmetric stretching, ν_s = symmetric stretching, δ = in–plane angular deformation.

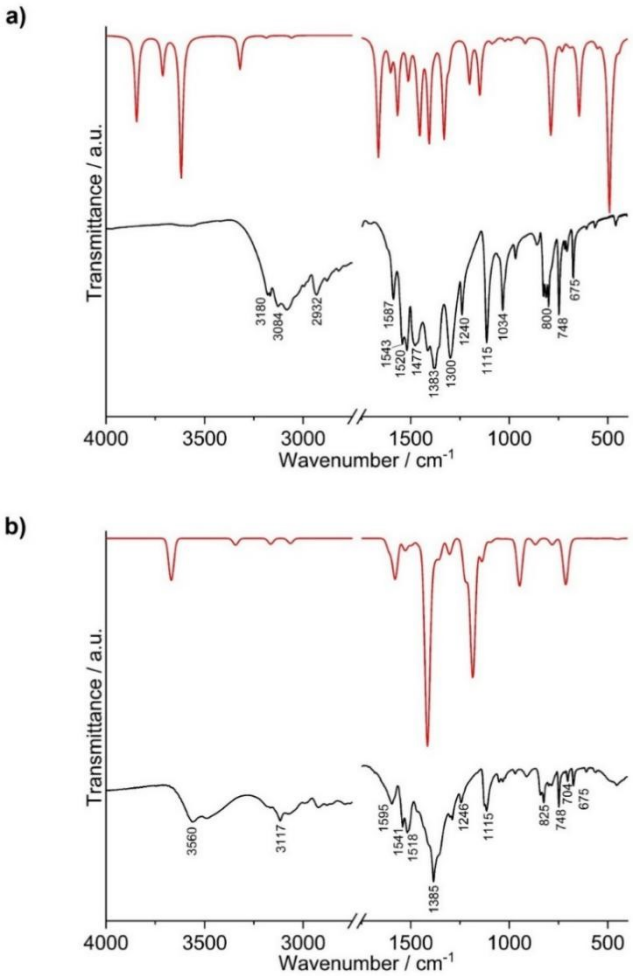

Figure S7. Experimental (black line) and calculated (red line) FTIR spectra for **(a)** $[Cu(2mni)_2(H_2O)_2](NO_3)_2(H_2O)_2$ (**1**) and **(b)** $[Cu(2mni)_2(NO_3)_2]$ (**2**).

Table S8. Tentative assignments for the Raman scattering spectra registered and calculated for products **1** and **2**

Tentative assignments	**1** Experimental	**1** Calculated	**2** Experimental	**2** Calculated
δ(N–H)	1542	1566	1545 and 1521	1577 and 1529
ν_{as}(N–O)	1461	1453	1460	1448
τ(CH)	1395 and 1373	1407 and 1379	1372	1381
β(CH)	1300	1306	1300	1303
ν(C–N)$_{ring}$	1241 and 1052	1222 and 1067	1238 and 1051	1222 and 1080
δ(C–N–C)	1118	1148	1118	1137
ν(C–C)$_{ring}$	1028 and 830	1021 and 919	1028 and 830	1034 and 867
δ(N–H)	742 and 708	732 and 700	745 and 709	741 and 714
ν(Cu–N)	563 and 456	553 and 442	562 and 450	555 and 451
ν(Cu–O)	309	308	311	314
Skeleton motions	≤400	–	≤400	–

ν = stretching, ν_{as} = asymmetric stretching, ν_s = symmetric stretching, δ = in–plane angular deformation, τ = out–of–plane bending (twisting), β = in–plane bending.

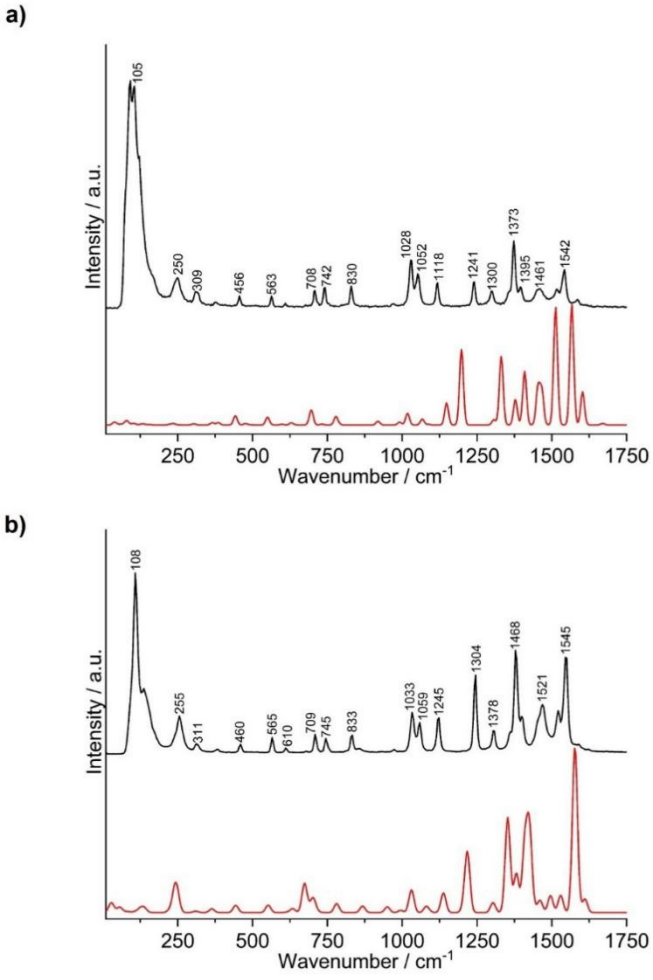

Figure S8. Experimental (black line) and calculated (red line) Raman spectra for **(a)** $[Cu(2mni)_2(H_2O)_2](NO_3)_2(H_2O)_2$ (**1**) and **(b)** $[Cu(2mni)_2(NO_3)_2]$ (**2**).

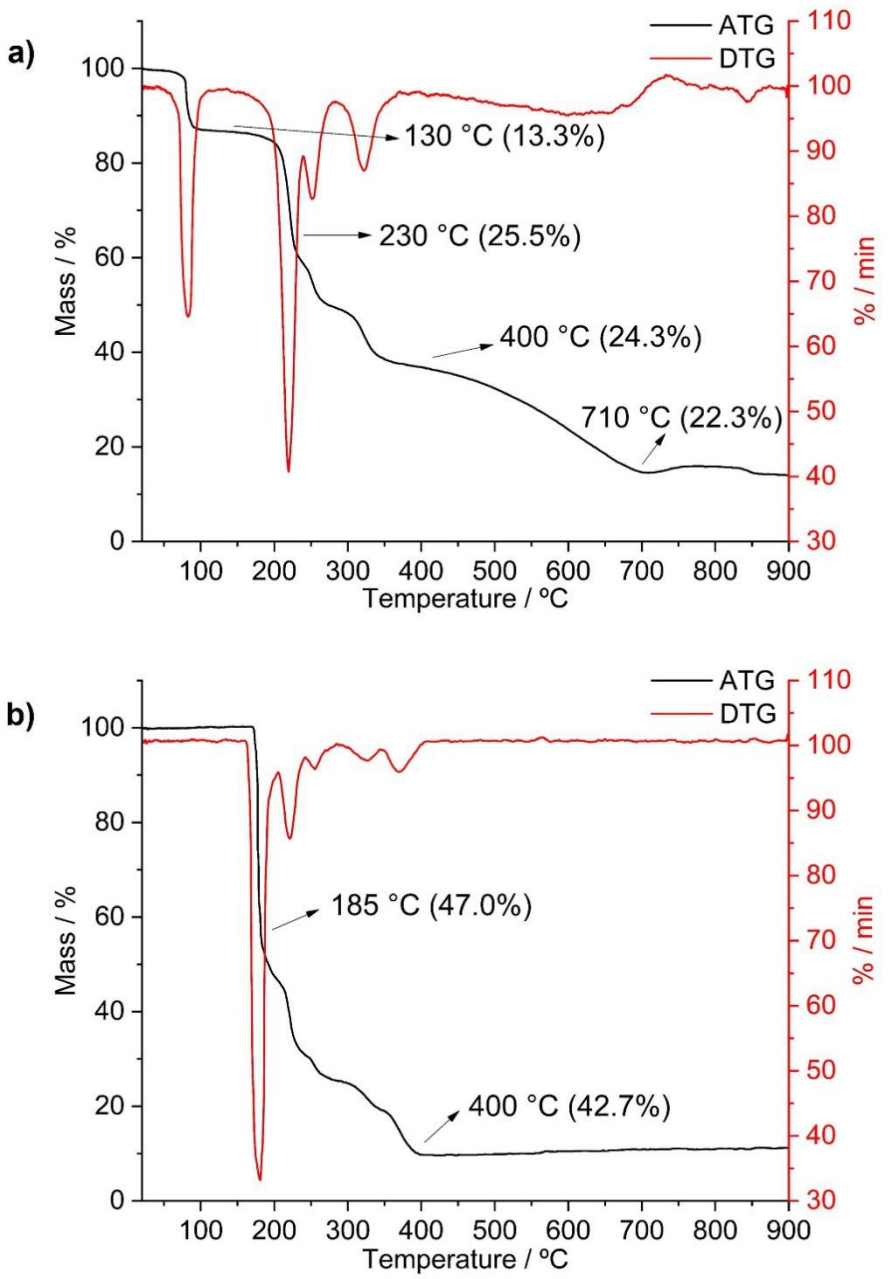

Figure S9. Thermogram and derivative thermogram (DTG, red) results for (a) product **1** and (b) **2** with the wieght loss steps evi denced. The thermograms were obtained in N_2/O_2 atmosphere and temperature range of 25 to 900 °C.

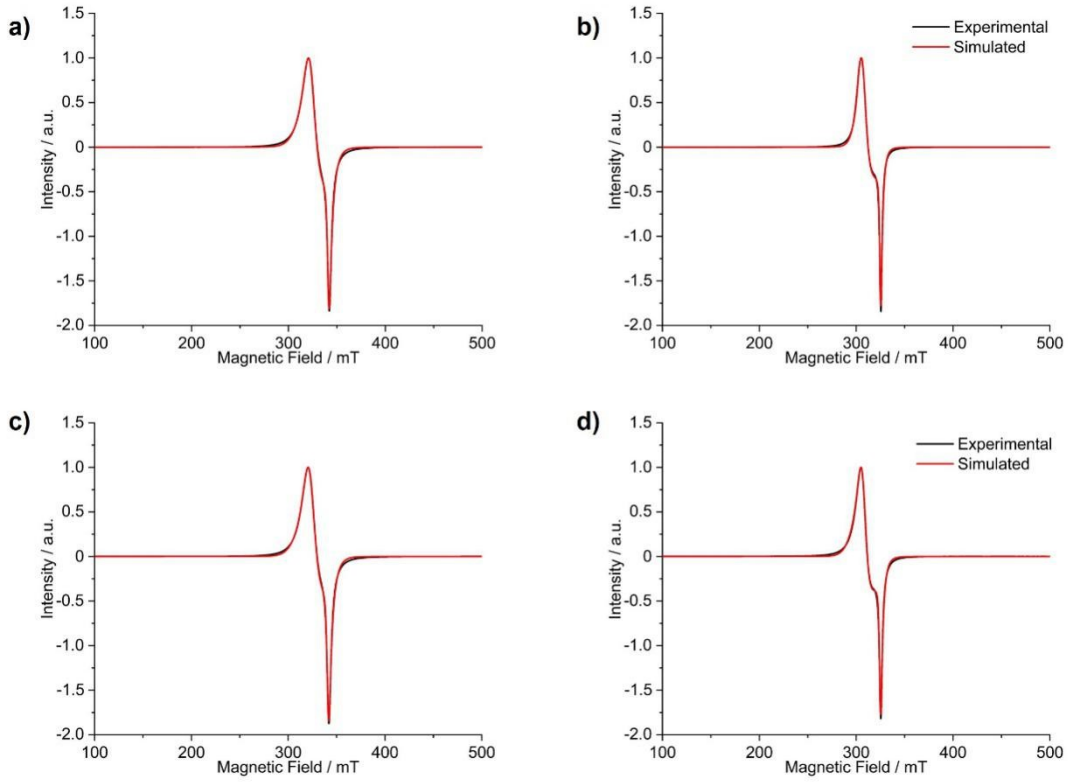

Figure S10. X-band EPR spectra in solid state at room temperature for *(a)* **1** and *(c)* **2**; and at 77 K for (b) **1** and (d) **2**. The experimental spectra are shown in black and the simulations run with EasySpin in red.

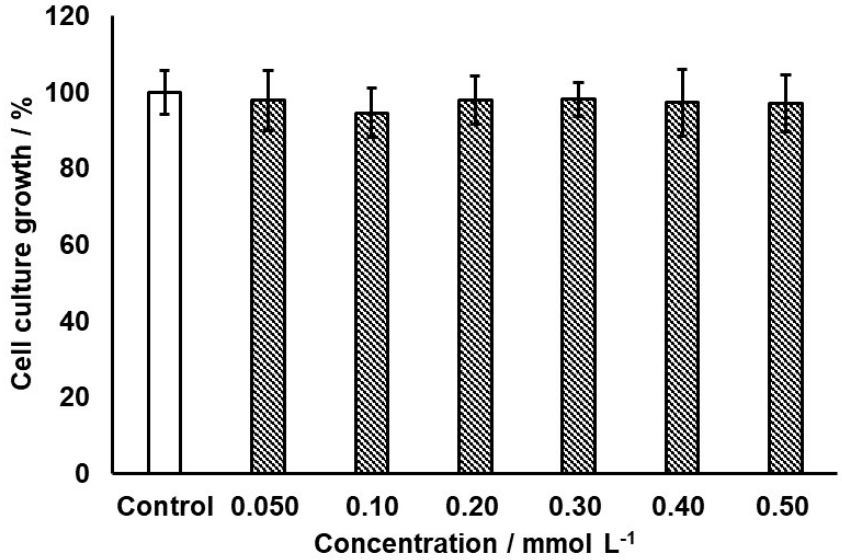

Figure S11. Growth inhibition assay in *E. coli* suspensions treated with 2-methyl-4(5)-nitroimidazole in concentrations from 0.050 to 0.50 mmol L^{-1}; Data were obtained after three hours of incubation at 37 °C and 120 rpm in triplicates and are given as average values and standard deviations. The OD_{595} value for the control was 0.930±0.068considered 100% of growth.

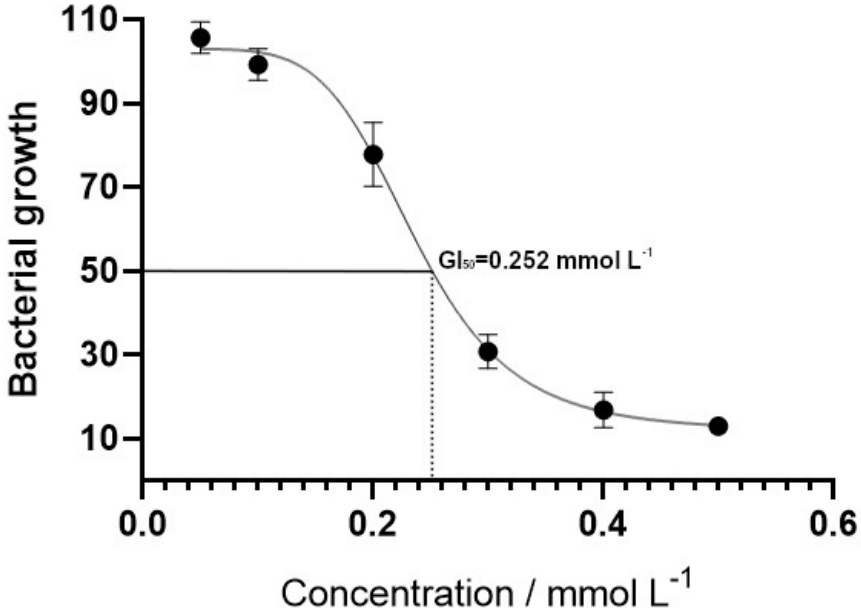

Figure S12. *E. coli* IC_{50} values determined in cytotoxicity essays with **1** in concentrations from 0.050 to 0.50 mmol L^{-1}, for 3 h. Data are presented as mean ±SD of three independent experiments. The solid lines represent the best fit curves as described in the Experimental section.

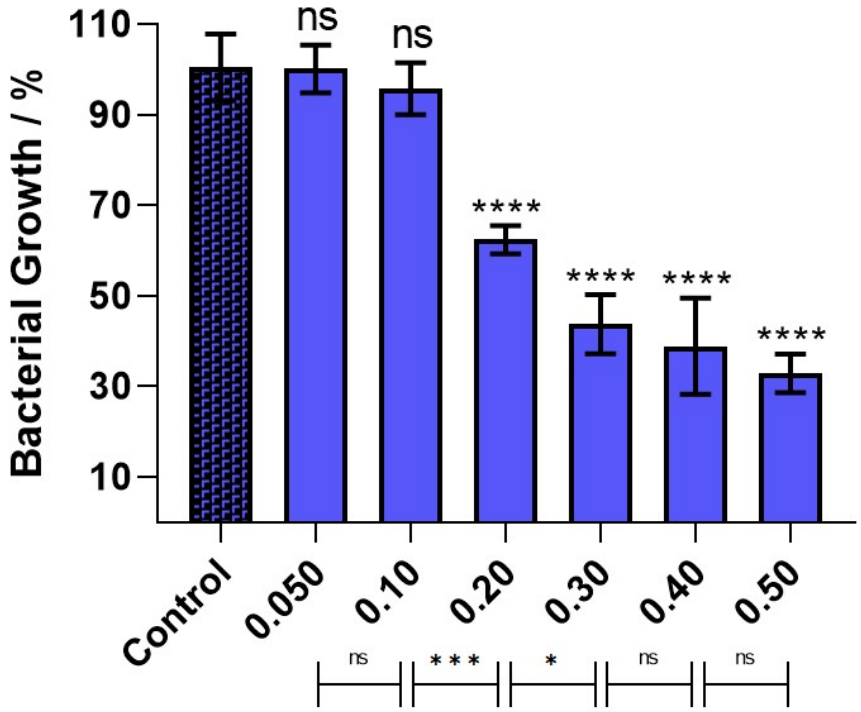

Figure S13. Growth inhibition assay in *E. coli* suspensions treated with copper nitrate in concentrations from 0.050 to 0.50 mmol L^{-1}; Data were obtained after three hours of incubation at 37 °C and 120 rpm in triplicates and are given as average values and standard deviations. ns = not statistically significant, **** = $p < 0.0001$ when compared to the control essay

REFERENCES

1. J. Montes-Ayala, C. Escartín-Guzmán, S. E. Castillo-Blum, E. O. Rodríguez-Hernández, S. Bernès, M. J. Rosales-Hoz and N. Barba-Behrens, *J Inorg Biochem*, 2005, **99**, 1676-1684.
2. J. R. Olson, M. Yamauchi and W. M. Butler, *Inorganica Chimica Acta*, 1985, **99**, 121-128.
3. C. Li, M. Zhang, Q. Chen, Y. Li, H. Gao, W. Fu and Z. Zhou, *Dalton Transactions*, 2016, **45**, 17956-17965.
4. J. Stierstorfer, K. R. Tarantik and T. M. Klapötke, *Chemistry – A European Journal*, 2009, **15**, 5775-5792.
5. G. Geisberger, T. M. Klapötke and J. Stierstorfer, *European Journal of Inorganic Chemistry*, 2007, **2007**, 4743-4750.
6. P. García-Holley, N. Ortiz-Pastrana, R. A. Toscano, M. Flores-Álamo and N. Barba-Behrens, *Polyhedron*, 2016, **104**, 127-137.